Sensors & Transducers, Vol. 156, Issue 9, September 2013, pp. 217-226

www.sensorsportal.com

Sensors & Transducers

http://www.sensorsportal.com

Computational-geometry-based Plant Organs Classification and Foliage 3D Reconstruction from Point Cloud Data

Ting Yun, Mingxing Gao, Yanming Wang, Xiaofeng Liu
Nanjing Forestry University, Longpan Road, No.159, Nanjing, 210037, China
Tel.: 13585100839, fax: 025-85427687
E-mail: njyunting@qq.com, liuxiaofeng.njfu@hotmail.com

Received: 5 June 2013 /Accepted: 25 August 2013 /Published: 30 September 2013

Abstract: In recent years Terrestrial Laser Scaner (TLS) is widely used in complex scene survey and space objects measurement, however, due to the trees' irregular and complex morphology, also the scanning results be effected by the wind blowing and occlusion effect, so quantifying the 3-D morphology structure and forestry index of an individual tree or a forest stand from Point Cloud Data (PCD) is a challenging task. In this paper, the computer theory is combined into our approach. Firstly the covariance matrixes based on neighborhood information are constructed to retrieve the feature vectors of every PCD, including normal vector, torsion and curvature from the scanning data. Secondly the LLE manifold-learning method is adopted for dimensionality reduction of PCD features, then identification and classification of different plant organs are achieved. Finally orthogonal least squares algorithm about three-dimensional surface fitting is presented to remove deviation caused by leaf jitter, then the whole PCD of singe leave are mapped onto one three-dimensional surface, next, many triangles are used to form the foliage area and Leaf Area Index (LAI) can be calculated based on the delaunay triangulation algorithm. In this paper we apply computer theory to overcome the shortcomings of TLS in forestry application, automatically and nondestructively achieve the classification of different plant organs and 3-D reconstruction of real foliage, most importantly, this work provide a theoretical foundation for retrieving LAI and forestry parameters from PCD obtained with a TLS. *Copyright © 2013 IFSA.*

Keywords: Terrestrial laser scanning (TLS), Point cloud data (PCD), Plant organs classification, Foliage 3-D reconstruction.

1. Introduction

The forest has an irreplaceable status in regulating the Earth's environment of human habitation and slowing down global environmental degradation trend, forest surveying and forestry information acquisition become an important issue in recent years, how to take fine measurement of quantitative forest inventories and provide an effective way to improve the accuracy and efficiency of forestry data collection is the main task in forestry management.

In recent years, there are several methods of obtaining trees morphology structure and measuring trees parameter. Firstly, plant canopy analyses and traditional mechanical instruments for trees measurement are inefficient and be affected by leaf overlap and aggregation, the measurement results also be influenced by sun zenith angle and mathematics calibration. Hyper-spectral remote

sensing [1, 2] measure the canopy from top down and usually include a recorded reflection from the ground, it is capable of producing one-shot topographic and spectral intensity information, which will enable a simultaneous study of structural and biochemical vegetation parameters, but hyper spectral instrument be affected by atmospheric conditions and accuracy of aerial photography, also it is not theoretically support by modern physical model. Airborne LIDAR [3, 4] can monitor plant biomass and growth, but if only rely on the finitely waveform of echo signal with attenuation and noise, we can not accurately estimate individual vegetation features. The TLS scans [5, 6] pulse laser over the full upper hemisphere and part of the lower hemisphere by using a mirror rotating in the vertical plane (the zenith scan) and a rotation of the instrument to provide azimuthal coverage. The time-dependent intensity of reflected light from each laser pulse is recorded, providing a waveform that may include responses from multiple targets. The laser produces an energy pulse that is distributed in time. The shape of the outgoing pulse is consistent and has a well defined peak. Reflections from targets are time-delayed copies of this pulse, where the range to the target is simply inferred from the arrival time of the pulse peak relative to the peak of the outgoing pulse. TLS can mosaic the multi-view scanning data, thereby ensure scanning data completeness and reduce the impact of foliage cover, eventually get 3D point cloud model of real stumpage. Due to high precision and high density characteristics of TLS, the TLS-based method is taken as a most appropriate method for tree measurement, it can also serve as a calibration tool for airborne laser scanning and other measurement application with ground sampling.

In recent years, there are several ideologies to calculate tree parameters from TLS point clouds.

1) Different space partitioning method and projection strategy about PCD are used to calculate vegetation architecture and foliage assemblage in each space cell, then to indicate trees' growth index [7, 8]. Such as Zheng [9] presented a new voxel-based method with line quadrat direction to retrieve the biophysical characteristics of the forest canopy including extinction coefficient, gap fraction, overlapping effect along the direction of the line quadrat and estimated effective leaf area (ELA) from TLS point cloud data. Bélanda [10] investigated the use of a voxel-based approach to retrieve leaf area distribution of individual trees from PCD and provided vertical as well as radial distributions of leaf area in individual trees to estimate savanna vegetation structural parameters with a high level of detail. Zheng [11] developed circular point cloud slicing to explore the spatial variation of point density for both azimuthal angular and radial directions; the result showed comprehensive scan combination could fully represent the canopy structure and structural variation of the heterogeneous forest stand.

2) The physical model and forestry formula are applied to PCD analyzing for forestry index calculation. Such as Lovella [12] used Semi-analytic Pgap and Radiative Transfer (CanSPART) model to predict tree gap probability (Pgap) profiles, then a canopy structure model based on simple geometric forms and parameterized with plot-scale statistical biometric data were used to predict gap probability (Pgap) profiles. Experimental result showed that his mathematical model about PCD calculation performs better in clumped canopies than a simple exponential model. Zheng [13] combined beer laws to present a new method that using total least square fitting techniques to reconstruct the normal vectors, then indirectly and nondestructively retrieved foliage elements' orientation and distribution from PCD obtained using a terrestrial laser scanning (TLS) approach.

3) Computer graphics and computer vision theory are studied for TLS point cloud processing. Xu [14] presented a semi-automatic method for realizing the sparse point clouds of range scanned trees transform to full polygonal models, a skeleton of the trunk and main branches was produced based on the scanned point clouds, then steps were taken to synthesize additional branches to produce plausible support for the tree crown, subsequently, allometric theory was used to estimate appropriate dimensions for each branch, at last, leaves were positioned, oriented and connected to nearby branches. Liang [15] presented a fully automatic stem-mapping algorithm, he used a series of cylinders to built up trees' stem model, result show in a relatively dense managed forest, the majority of stems could be located by proposed automatic algorithm.

In summary, three questions are existed in tree's LAI calculation:

1) How to extracted and distinguished the leaf from the flourishing tree's PCD with enormous various leaf inclination angle and morphology.

2) The scanning PCD exist deviation and jitter due to disturbance and occlusion of external environmental conditions, so how to remove the measurement deviation and design the algorithm to get real deformation foliage data is to be considered.

3) TLS can obtain discrete point cloud data, while the manifestation of real leaves is in the form of three dimensional surfaces, so how to design a reasonable point to plane transform algorithm is to be solved.

Due to extreme complex morphology of trees, in order to retrieve the biophysical characteristics of real stumpage including LAI, branches location, crown density, tree trunk shape etc, it needs the combination of computer vision and graphics theory to explore hidden information from PCD. In this paper the manifold learning LLE method is adopted to classify and identify different tree organs, then the least squares surface fitting method with orthogonal distance is proposed to eliminate deviation which caused by wind and occlusion, then PCD projection on the Z axis without spatial morphology distortion is achieved. Finally,

triangulation algorithm for foliage modeling is designed to derive real tree leave 3D model.

2. Plant Organs Classification Based on Manifold Learning

2.1. Characteristics of PCD Calculation

In this section, the spatial distribution properties of the laser points are studied. Trees' PCD are defined by means of features calculation such as flatness, direction, and shape. Due to geometrical form difference, different organs of trees share dissimilar attributes, therefore, a robust feature extraction and classification method is needed to estimate stumpage parameters when branches or foliages points are present. In this step, the properties of point distribution, such as flatness and normal vector direction, are used to distinguish the trees' organs from the huge amounts of irregular PCD. Consequently, the method about feature calculation is given below.

For a point $p_i = (x_i, y_i, z_i)^T$ in the point cloud P, $P \subset R^3$, its surrounding finite space is defined by N nearest points $p_j = (x_j, y_j, z_j)^T$ with mean $u = (1/N)\sum_{j=1}^{N} p_j$, the covariance matrix C_P of points p_j is defined by $C_p = \frac{1}{N}\sum_{j=1}^{N}(p_j - u)(p_j - u)^T$, the point set p_j itself does not have context information. The eigenvalue & eigenvector approach is usually employed to study point distribution, by utilizing eigenvalue decomposition, a new coordinate system can be defined, where point directions are given by eigenvectors and point variances along axes are given by the corresponding eigenvalues. Let e_i be the eigenvector and λ_i be the corresponding eigenvalue, where $i = 0,1,2,..$ and $\lambda_0 \le \lambda_1 \le \lambda_2$. In this new coordinate system, e_0 gives the direction in which the points exhibit the least variance and e_2 gives the one in which the points exhibit the most variance. Where a surface structure is spanned in the neighborhood, e_0 approximates the normal vector at point p_i. For convenience, e_0 is denoted as the normal vector in the following. The eigenvalue λ_i quantitatively shows the data variance along the axis e_i, or the compactness of the point distribution along the axis. Therefore, flatness F_l can be defined as $F_l = 1 - \frac{\lambda_0}{\lambda_0 + \lambda_1 + \lambda_2}$, which shows the significance of the point distribution in two main directions. A high value of F_l means that the point is approximately on a planar surface.

After the above analysis, a series of features about each point p_i is obtained, described as $c_{pi} = \{x_i, y_i, z_i, r_i, g_i, b_i, e_{ix}, e_{iy}, e_{iz}\}$, where r_i, g_i, b_i is the color value and e_{ix}, e_{iy}, e_{iz} represent the normal vector of p_i, then these features are taken into the classification algorithm to realize different tree organs classification.

2.2. PCD Classification Based on LLE Framework

LLE [16] maps a data set $C_p = \{c_{p1}, c_{p2}, c_{p3}, ...c_{pn}\}$, $c_{pi} \in R_d$ globally to a data set $Y = \{y_1, y_2, y_3, ...y_n\}$, $y_i \in R^m$. In previous section calculating c_{pi} has been described, assuming the data lies on a nonlinear manifold which locally can be approximated linearly, it uses two stages:

1) locally fitting hyper planes around each sample c_{pi}, based on k nearest neighbors of point p_i, and calculating reconstruction weights;

2) finding lower dimensional co-ordinates y_i for each c_{pi}, by minimizing a mapping function based on these weights. In stage 1, the cost function minimized is:

$$\min \varepsilon(W) = \sum_{i=1}^{n} \left| c_{pi} - \sum_{j=1}^{k} w_j^i c_{pN(j)} \right|^2 \quad (1)$$

i.e. how well each p_i can be linearly reconstructed in terms of its neighbors $p_{N(1)}$ $p_{N(2)} \cdots p_{N(k)}$. For one vector c_{pi} and weights $w_j^{(i)}$ that sum up to 1, this gives a contribution

$$\varepsilon_I(W) = \left| \sum_{j=1}^{k} w_j^{(i)} \left(c_{pi} - c_{pN(j)} \right) \right|^2 = \sum_{j=1}^{k}\sum_{m=1}^{k} w_j^{(i)} w_m^{(i)} Q_{jm}^{(i)}, \quad (2)$$

where $Q^{(i)}$ is the $k \times k$ matrix

$$Q_{jm}^{(i)} = \left(c_{pi} - c_{pN(j)} \right)^T \left(c_{pi} - c_{pN(m)} \right) \quad (3)$$

Let $R^{(i)} = \left(Q^{(i)} \right)^{-1}$. Solving the least squares problem (Eq. (2)) with constraint $\sum_j w_j^{(i)} = 1$ gives:

$$w_j^{(i)} = \sum_{m=1}^{k} R_{jm}^{(i)} \Big/ \sum_{p=1}^{k}\sum_{q=1}^{k} R_{pq}^{(i)} \quad (4)$$

In practice, a regularization parameter r will have to be used for $Q^{(i)}$ before inversion (as its rank is d, certainly for $k > d$): $R^{(i)} = \left(Q^{(i)} + rI \right)^{-1}$.

Interestingly, $Q^{(i)}$ can also be calculated based on just the squared Euclidean distance matrix D between all samples in C_p:

$$Q_{jm}^{(i)} = \frac{1}{2}\left(D_{i,N(j)} + D_{i,N(m)} - D_{N(j),N(m)}\right) \quad (5)$$

In stage II, the weights w are fixed and new m-dimensional vectors y_i are sought which minimize the criterion:

$$\min \varepsilon_{\Pi}(Y) = \sum_{i=1}^{n}\left|y_i - \sum_{j=1}^{k} w_j^{(i)} y_{N(j)}\right|^2 \quad (6)$$

The $w_j^{(i)}$ can be stored in a $n \times n$ sparse matrix W, where $W_{i,N(j)} = w_j^{(i)}$. Re-writing Eq. (6) then gives

$$\varepsilon_{\Pi}(Y) = \sum_{i=1}^{n}\sum_{j=1}^{n} M_{ij} y_i^T y_j = tr\left(YMY^T\right), \quad (7)$$

where M is an $n \times n$ matrix found as $M = (I-W)^T(I-W)$ and Y contains the y_i's as its columns. To be able to solve this problem, the covariance matrix of the y's can be constrained to be identity. Finding Y then becomes a well-known problem: minimize $tr\left(YMY^T\right)$ with constraint $\frac{1}{n}YY^T = I$. All eigenvectors of M are solutions, the eigenvector with the smallest eigenvalue corresponds to the mean of Y and can be discarded to enforce $\sum_{i=1}^{n} y_i = 0$. The next m eigenvectors then give the Y that minimizes Eq. (7).

By LLE classification, the high dimensional PCD can be projected to a low-dimensional plane, on this plane we take finely classification according to the data distribution and distinguish the different plant organs through back projection to the original high dimension data space. In this way, classification and identification of one tree's PCD have finished, then, the results prepare for leaf three dimensional modeling.

3. Foliage Reconstruction Using Orthogonal Least Squares Fitting and Delaunay Triangulation Algorithm

3.1. Surface Fitting Based on Least Squares Method

The method of least squares requires that the vertical distance from each observed data point to the model surface be such that the sum of the squares of these distances is a minimum.

Given the data set:, $\{(x_1,y_1,z_1), (x_2,y_2,z_2),..., (x_n,y_n,z_n)\}$ calculate coefficients $a_1, a_2, ...a_m$ in the fitting equation of quadric surface:

$$f_3(l_i) = f_3(x,y) = a_1 + a_2x + a_3y + a_4x^2 + a_5xy + a_6y^2 + a_7x^3 + a_8x^2y + a_9xy^2 + a_{10}y^3 \qquad j = 1,2..,10. \quad (8)$$

and the fitting equation of cubic surface is described as:

$$f_2(l_i) = f_2(x,y) = a_1 + a_2x + a_3y + a_4x^2 + a_5xy + a_6y^2, \quad (9)$$

where $l_i = (x_i, y_i)$, so the sum of squared errors

$$E(f) = \sum_{i=1}^{n}\left(f(l_i) - z_i\right)^2 = \sum_{i=1}^{n}\left(\sum_{j=1}^{m} a_j f(l_i) - z_i\right)^2 \quad (10)$$

is minimized. Then set up the equations:

$$\partial E(f)/\partial a_j = 0 \quad j = 1,2,...,m \quad (11)$$

Re-writing Eq. (8) then gives

$$\begin{aligned}\frac{\partial E(f)}{\partial a_j} &= 2\sum_{i=1}^{n}\frac{\partial f(l_i)}{\partial a_j}\left[f(l_i) - z_i\right] = 2\sum_{i=1}^{n} b_i^j\left[f(l_i) - z_i\right] = 0 \\ &= 2\sum_{i=1}^{n}\left[b_i^j\left(a_1b_i^1 + a_2b_i^2 + ... + a_mb_i^m\right) - b_i^j z_i\right] \\ &= 2\left[a_1\left(\sum_{i=1}^{n} b_i^j b_i^1\right) + a_2\left(\sum_{i=1}^{n} b_i^j b_i^2\right) + ... + a_m\left(\sum_{i=1}^{n} b_i^j b_i^m\right) - \left(\sum_{i=1}^{n} b_i^j z_i\right)\right]\end{aligned} \quad (12)$$

Solve for the coefficients $a_1, a_2, ..., a_m$, the Eq. (12) becomes

$$\begin{cases} a_1\sum_{i=1}^{n} b_i^1 b_i^1 + a_2\sum_{i=1}^{n} b_i^1 b_i^2 + ... + a_m\sum_{i=1}^{n} b_i^1 b_i^m = \sum_{i=1}^{n} b_i^1 z_i \\ a_1\sum_{i=1}^{n} b_i^2 b_i^1 + a_2\sum_{i=1}^{n} b_i^2 b_i^2 + ... + a_m\sum_{i=1}^{n} b_i^2 b_i^m = \sum_{i=1}^{n} b_i^2 z_i \\ ... \\ a_1\sum_{i=1}^{n} b_i^m b_i^1 + a_2\sum_{i=1}^{n} b_i^m b_i^2 + ... + a_m\sum_{i=1}^{n} b_i^m b_i^m = \sum_{i=1}^{n} b_i^m z_i \end{cases} \quad (13)$$

Eq. (13) gives in matrix notation $BB^TA = BZ$, where $B = \begin{bmatrix} b^1(l_1) & b^1(l_2) & ... & b^1(l_n) \\ b^2(l_1) & b^2(l_2) & ... & b^2(l_n) \\ & & \vdots & \\ b^m(l_1) & b^m(l_2) & & b^m(l_n) \end{bmatrix}$

$A^T = (a_1, a_2, ..., a_m)$, $Z^T = (z_1, z_2, ..., z_n)$, B is the $m \times n$ matrix, A and Z are the m, n vector. Based on the above matrix equation, the value of $a_1, a_2, ..., a_n$ can be estimated, then least squares method is finished.

3.2. The Least Squares Surface Fitting Method Using Orthogonal Distance

In this section we introduce our very efficient orthogonal distance fitting algorithm for implicit surfaces, the orthogonal distance or the modifications between measurement points to the fitting surface is

$$\begin{cases} x_p = x_p^0 + \delta_{x_p} \\ y_p = y_p^0 + \delta_{y_p} \\ a_{ij} = a_{ij}^0 + \delta_{c_{ij}} \end{cases} \tag{14}$$

δ represents correction coefficient, Eq. (14) is equivalent to

$$\begin{cases} v_{xp} = \delta_{x_p} + x_p - x_p^0 \\ v_{yp} = \delta_{y_p} + y_p - y_p^0 \\ v_{zp} = \sum_{i=0}^{m} \sum_{j=0}^{m-i} \left(a_{ij} x_p^i y_p^j - z_p^0 \right) \end{cases} \tag{15}$$

From Eq. (14) and Eq. (15), we get

$$\begin{cases} v_{xp} = \delta_{x_p} + x_p - x_p^0 \\ v_{yp} = \delta_{y_p} + y_p - y_p^0 \\ v_{zp} = \sum_{i=0}^{m} \sum_{j=0}^{m-i} \left(a_{ij}^0 + \delta_{c_{ij}} \right) \left(x_p^0 + \delta_{x_p} \right)^i \left(y_p^0 + \delta_{y_p} \right)^j - z_p^0 \end{cases} \tag{16}$$

After Eq. (16) expansion, we obtained

$$\begin{cases} v_{xp} = \delta_{x_p} + x_p - x_p^0 \\ v_{yp} = \delta_{y_p} + y_p - y_p^0 \\ v_{zp} = \sum_{i=0}^{m} \sum_{j=0}^{m-i} \left\{ \left(a_{ij}^0 + \delta_{c_{ij}} \right) \left[\left(x_p^0 \right)^i + i \left(x_p^0 \right)^{i-1} \delta_{x_p} + \left(\delta_{x_p} \right)^i \right] \right. \\ \left. \left[\left(y_p^0 \right)^j + j \left(y_p^0 \right)^{j-1} \delta_{y_p} + \left(\delta_{y_p} \right)^j \right] - z_p^0 \right\} \end{cases} \tag{17}$$

through calculation then get

$$\begin{cases} v_{xp} = \delta_{x_p} + x_p - x_p^0 \\ v_{yp} = \delta_{y_p} + y_p - y_p^0 \\ v_{zp} = \sum_{i=0}^{m} \sum_{j=0}^{m-i} \left\{ \left(a_{ij}^0 + \delta_{c_{ij}} \right) \left[\left(x_p^0 \right)^i \left(y_p^0 \right)^j + i \left(x_p^0 \right)^{i-1} \delta_{x_p} \left(y_p^0 \right)^j + \right. \right. \\ \left. \left. j \left(y_p^0 \right)^{j-1} \delta_{y_p} \left(x_p^0 \right)^i + i \left(x_p^0 \right)^{i-1} \delta_{x_p} j \left(y_p^0 \right)^{j-1} \delta_{y_p} + \left(\delta_{x_p} \right)^i \left(\delta_{y_p} \right)^j \right] - z_p^0 \right\} \end{cases} \tag{18}$$

In Eq. (18), the item including $(\delta)^n \; n \geq 2$ can be discarded because δ is a small offset value, so the power of δ can be ignored. Then derivatives of Eq. (18) lead to

$$\begin{cases} v_{xp} = \delta_{x_p} + x_p - x_p^0 \\ v_{yp} = \delta_{y_p} + y_p - y_p^0 \\ v_{zp} = \sum_{i=0}^{m} \sum_{j=0}^{m-i} a_{ij}^0 \left(x_p^0 \right)^i \left(y_p^0 \right)^j + a_{ij}^0 i \left(x_p^0 \right)^{i-1} \delta_{x_p} \left(y_p^0 \right)^j \\ + a_{ij}^0 j \left(y_p^0 \right)^{j-1} \delta_{y_p} \left(x_p^0 \right)^i + \delta_{c_{ij}} \left(x_p^0 \right)^i \left(y_p^0 \right)^j - z_p^0 \end{cases} \tag{19}$$

The matrix form of Eq. (19) is described as:

$$V = \begin{bmatrix} I_{x_p} & 0 & 0 \\ 0 & I_{y_p} & 0 \\ B_x & B_y & J \end{bmatrix} \begin{bmatrix} \delta_{x_p} \\ \delta_{y_p} \\ \delta_{c_{ij}} \end{bmatrix} + \begin{bmatrix} L_1 \\ L_2 \\ L_3 \end{bmatrix} = GX + L , \tag{20}$$

where I_{x_p}, I_{y_p} are identity matrix with p dimension, B_x, B_y are diagonal matrix with p dimension,

$$B_x = \begin{bmatrix} \sum_{i=0}^{m} \sum_{j=0}^{m-i} i \left(x_1^0 \right)^{i-1} \left(y_1^0 \right)^j a_{ij}, 0, ..., 0 \\ 0, \sum_{i=0}^{m} \sum_{j=0}^{m-i} i \left(x_2^0 \right)^{i-1} \left(y_2^0 \right)^j a_{ij}, ..., 0 \\ 0, 0, ..., \qquad 0 \\ 0, 0, ..., \sum_{i=0}^{m} \sum_{j=0}^{m-i} i \left(x_n^0 \right)^{i-1} \left(y_n^0 \right)^j a_{ij} \end{bmatrix}$$

$$B_y = \begin{bmatrix} \sum_{i=0}^{m} \sum_{j=0}^{m-i} j \left(y_1^0 \right)^{j-1} \left(x_1^0 \right)^i a_{ij}, 0, ..., 0 \\ 0, \sum_{i=0}^{m} \sum_{j=0}^{m-i} i \left(y_2^0 \right)^{j-1} \left(x_2^0 \right)^i a_{ij}, ..., 0 \\ 0, 0, ..., \qquad 0 \\ 0, 0, ..., \sum_{i=0}^{m} \sum_{j=0}^{m-i} i \left(y_p^0 \right)^{j-1} \left(x_p^0 \right)^i a_{ij} \end{bmatrix}$$

$$J = \begin{bmatrix} \sum_{i=0}^{m} \sum_{j=0}^{m-i} \left(x_1^0 \right)^i \left(y_1^0 \right)^j \\ \sum_{i=0}^{m} \sum_{j=0}^{m-i} \left(x_2^0 \right)^i \left(y_2^0 \right)^j \\ ... \\ \sum_{i=0}^{m} \sum_{j=0}^{m-i} \left(x_p^0 \right)^i \left(y_p^0 \right)^j \end{bmatrix}$$

$$L = \begin{bmatrix} x_p - x_p^0 = 0 \\ y_p - y_p^0 = 0 \\ a_{ij} \left(x_p^0 \right)^i \left(y_p^0 \right)^j - z_p^0 \end{bmatrix}$$

The indirect adjustment method is used to minimize the Eq. (20), then get $\delta = \left(G^T G \right)^{-1} G^T L$. Bring the δ into the Eq. (14), the fitting surface answer is

$$z_p = \sum_{i=0}^{m} \sum_{j=0}^{m-i} \left(a_{ij} x_p^i y_p^j \right) \quad (21)$$

Through orthogonal least square fitting method, we can get jitter-free and non interference real leaves PCD, based on this; the triangulation algorithm is adopted to accomplish the conversion of discrete points to foliage surface.

4. Experimental Results

4.1. Experimental 1

We first collect a scan of a well-isolated individual tree, scanned from two side lateral locations, this preliminary data set is used to develop and illustrate the algorithm. The upper portion of the complete individual big-leaf tree's PCD is provided for our experiment, shown in Fig. 1 (a). The leaf orientation distribution and the direction of a solid angle originated from every PCD are shown in Fig. 1 (b). Fig. 1 (c) shows that K-means clustering of partitioning method are used, through this method; we examine similarities and dissimilarities of observations PCD, where the characteristics of points in the same cluster are same color and the characteristics of points in different clusters are presented by different color. Seen from the Fig. 1 (c) the existing K-means clustering method can not effectively classify the plant organs; In Fig. 1 (d), curve drawing and description are adopted to analyze every inter-class variance, where curves of different colors represent different classes feature quantity, the black thick line represents the average value of this class. As seen from Fig. 1 (d), the curve of every class exist significant fluctuation and indicate the classification results are not optimal. Fig. 1 (e) shows the building low dimensional embedded space of the tree's PCD by the manifold learning LLE algorithm, we find a low dimensional basis for describing high dimensional tree PCD, then uncover the intrinsic dimensionality of the PCD. Fig. 1 (e) convert to the Fig. 1 (f) of three-dimensional space, in the Fig. 1 (f) XOY plane is corresponding with Fig. 1 (e), the Z axis keep the count of projective PCD numbers on the Fig. 1 (e) plane, through the selection of threshold value, classification results of tree's PCD are determined. Fig. 1 (g) shows the classification results of manifold learning LLE algorithm, as seen from the result, our method be able to identify different plant organs. It's clear from Fig. 1 (h) that each species have discernibly same characteristic quantity and every cluster characteristics are similar to its cluster centroid.

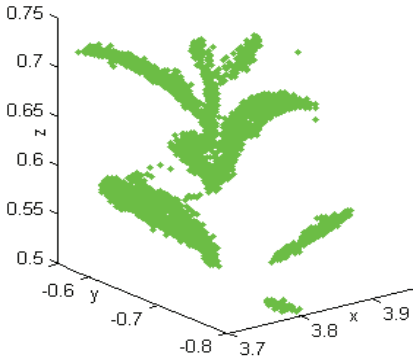

(a)

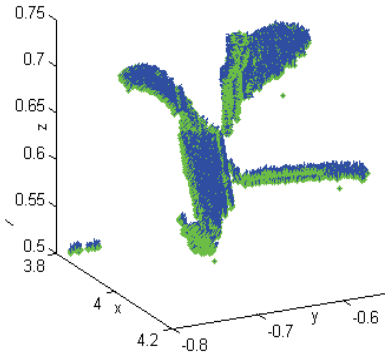

(b)

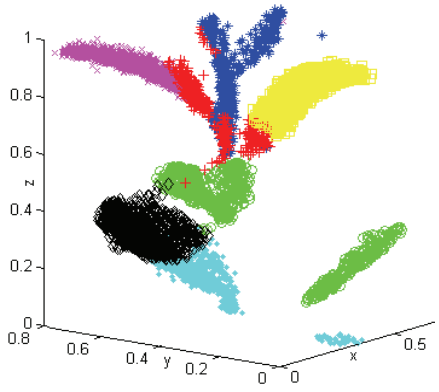

(c)

Fig. 1 (a-c). The classification result of different algorithm.

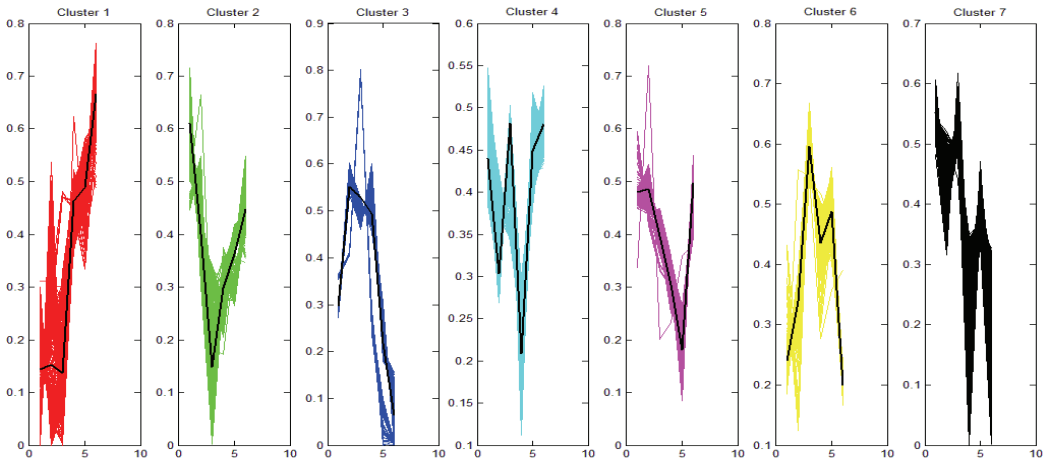

(d)

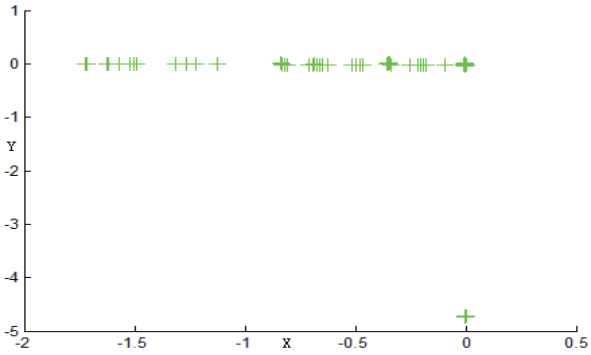

(e)

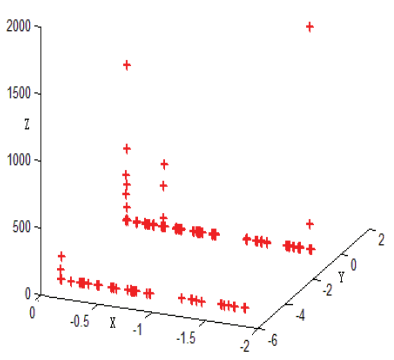

(f)

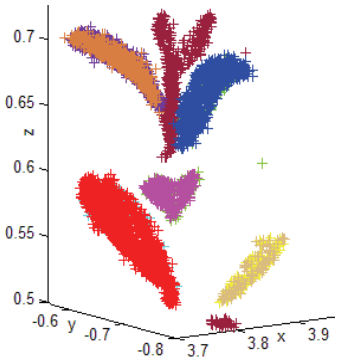

(g)

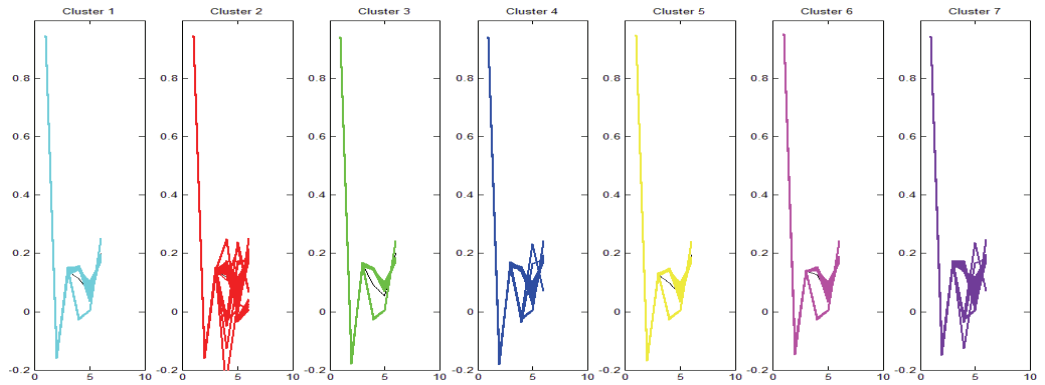

(h)

Fig. 1 (d-h). The classification result of different algorithm.

4.2. Experimental 2

Fig. 2 Schematic diagrams illustrate the tree leaves modeling process; Fig. 2 (a) Original PCD of an individual tree leaf; Fig. 2 (b) shows the fitting leaf surface after curve fitting method from PCD; we can see from Fig. 2 (c) that the fitting results by the curve fitting method can not construct a surface because an arbitrary surface can not contain all the leaf PCD, so the least squares estimation and orthogonal least square method are used to map all the PCD onto the approximating surface, the results are shown in Fig. 2 (d), Fig. 2 (e), Fig. 2 (f), where the red points represent the original foliar PCD, the green points represent the results of original foliar PCD taking "projection" operation by least square approach, the blue points are the "projection" operation results by orthogonal least square method; Fig. 2 (g), Fig. 2 (h) describe the projection surface through least square approach and orthogonal least square method, just express in the color of black and pink, then we obtain a set of projection vertices about original foliar PCD at the projection surface and utilize delaunay triangulation algorithm to generate triangle meshes with highly quality (Fig. 2 (i)), finally, adaptive subdivision and mesh re-sampling based on distance field are provided (Fig. 2 (j), Fig. 2 (k)).

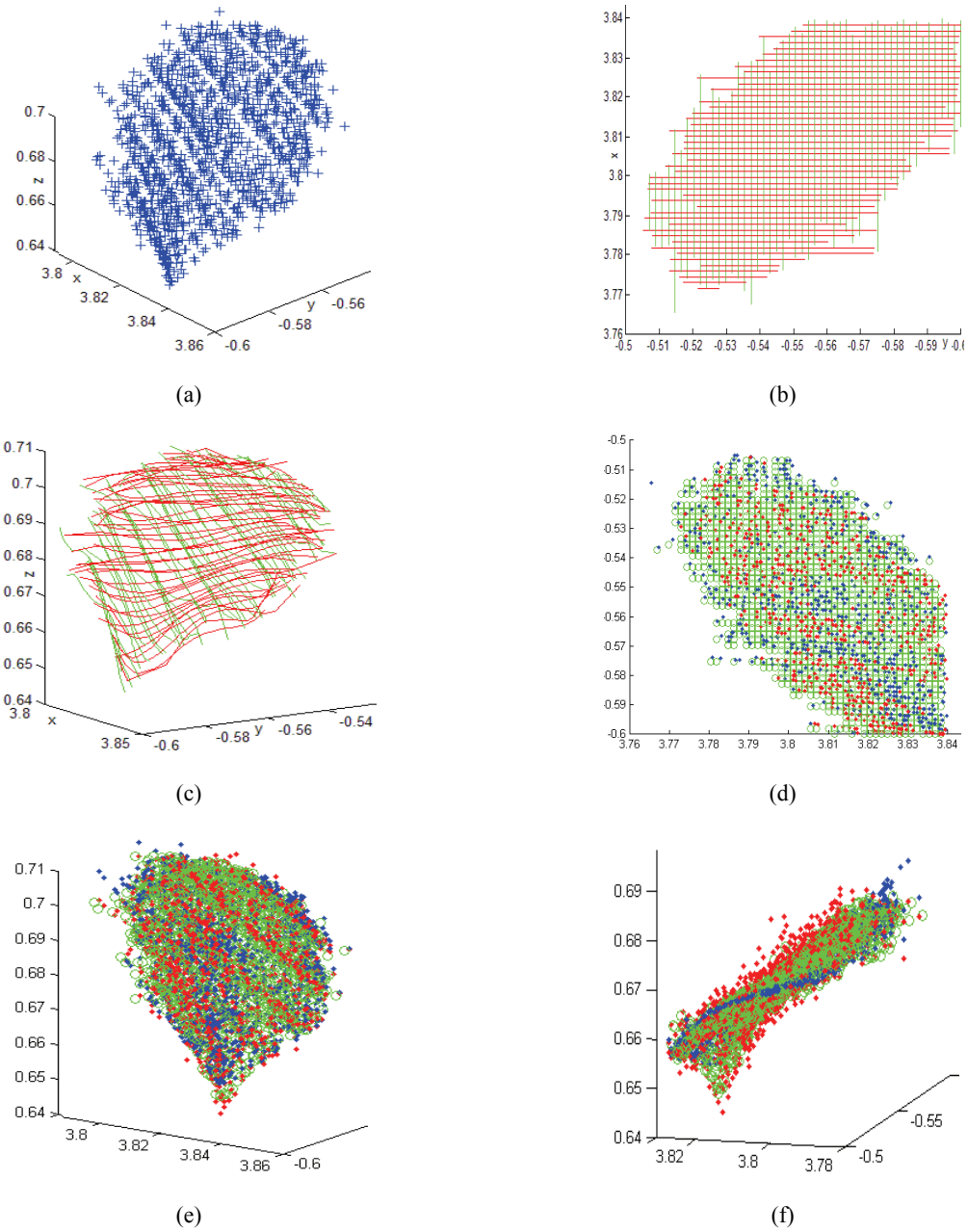

Fig. 2 (a-f). The experiment result of foliage reconstruction.

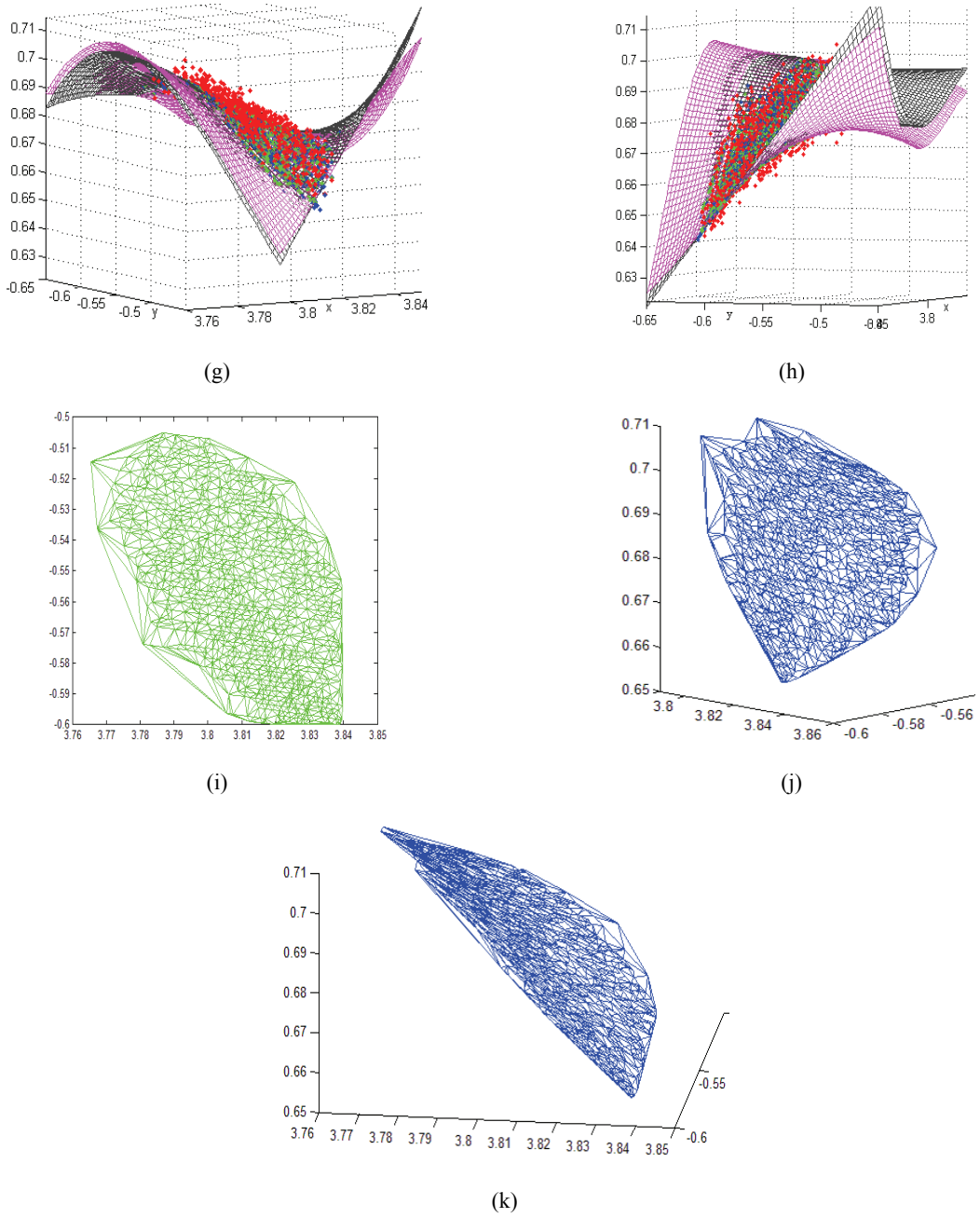

Fig. 2 (g-k). The experiment result of foliage reconstruction.

5. Conclusions

In recent years, TLS has been used in forestry parameter measurement, but the stumpage shape is non-rigid and irregular, and the scanning results are interfered by external environment, such as wind and occlusion effect, so the registration of multi-location scanning PCD exist deviation and can not fully capture 3-D structural information of forest stands. In this paper, we combine computer graphics and vision theory to provide a novel non-contact way for trees parameters calculation and real three dimension construction, our work mainly include:

1) Using the point and its neighborhood, we construct the covariance matrix to calculate the normal vector of every point, and take color information, torsion, curvature to form multi-dimensional characteristics of PCD.

2) Nonlinear manifold learning method is explored for dimensionality reduction of the tree's PCD features and plant organs identification.

3) Due to foliar jitter caused by the wind, three-dimensional orthogonal least squares algorithm is designed to eliminate jitter, thus making the whole leaf's PCD can project onto single surface and obtain the real leaves surface, then delaunay triangulation algorithm is used to realize the conversion between the discrete PCD to the real leave surface.

In brief, this paper use the latest measurement technology (TLS) to extend traditional tree index acquisition method, and combine computer science to identify different leaves organs, then proceed to

achieve leaf surface reconstruction. After this subject study, the mode innovation of broad-leaved trees measurement is proposed and the construction of forestry digitization process is developed.

Acknowledgements

This work is supported by natural science foundation of Jiangsu Province (BK2012418), High academic qualifications fund of Nanjing Forestry University (163070052, 163070036). We also appreciate Advanced Analysis and Testing Center of Nanjing Forestry University that provide the Leica TLS for our measurement.

References

[1]. S. Hancock, P. Lewisb, M. Fosterd, et al., Measuring forests with dual wavelength lidar: A simulation study over topography, *Agricultural and Forest Meteorology*, Vol. 161, Aug. 2012, pp. 123-133.

[2]. B. Koch, Status and future of laser scanning, synthetic aperture radar and hyperspectral remote sensing data for forest biomass assessment, *ISPRS Journal of Photogrammetry and Remote Sensing*, Vol. 65, Issue 6, Nov. 2010, pp. 581-590.

[3]. A. Ferraz, F. Bretar, S. Jacquemoud, et al., 3-D mapping of a multi-layered Mediterranean forest using ALS data, *Remote Sensing of Environment*, Vol. 121, Jun. 2012, pp. 210–223.

[4]. A. Peduzzi, H. R. Wynne, T. R. Fox, et al., Estimating leaf area index in intensively managed pine plantations using airborne laser scanner data, *Forest Ecology and Management*, Vol. 270, Apr. 2012, pp. 54-65.

[5]. D. Seidela, S. Fleckb, C. Leuschner, Analyzing forest canopies with ground-based laser scanning: A comparison with hemispherical photography, *Agricultural and Forest Meteorology*, Vol. 154, Mar. 2012, pp. 1-8.

[6]. J. L. Lovell, D. L. B. Jupp, G. J. Newnhamc, et al., Measuring tree stem diameters using intensity profiles from ground-based scanning lidar from a fixed viewpoint, *ISPRS Journal of Photogrammetry and Remote Sensing*, Vol. 66, Issue 1, Jan. 2011, pp. 46-55.

[7]. I. Moorthya, J. R. Miller, B. Hu, et al., Field characterization of olive (Olea europaea L.) tree crown architecture using terrestrial laser scanning data, *Agricultural and Forest Meteorology*, Vol. 151, Issue 2, Nov. 2011, pp. 204-214.

[8]. A. Iio, Y. Kakubari, H. Mizunaga, A three-dimensional light transfer model based on the vertical point-quadrant method and Monte-Carlo simulation in a Fagus crenata forest canopy on Mount Naeba in Japan, *Agricultural and Forest Meteorology*, Vol. 151, Issue 4, Apr. 2011, pp. 461-479.

[9]. G. Zheng, L. Monika Moskal, Computational-Geometry-Based Retrieval of Effective Leaf Area Index Using Terrestrial Laser Scanning, *IEEE Transactions On Geoscience and Remote Sensing*, Vol. 50, Issue 10, Oct. 2012, pp. 3958-3969.

[10]. M. Bélanda, J. L. Widlowskib, R. A. Fourniera, Estimating leaf area distribution in savanna trees from terrestrial LiDAR Measurements, *Agricultural and Forest Meteorology*, Vol. 151, Issue 5, Sep. 2011. pp. 1252-1266.

[11]. G. Zheng, L. Monika Moskal, Spatial variability of terrestrial laser scanning based leaf area index, *International Journal of Applied Earth Observation and Geoinformation*, Vol. 19, Oct. 2012. pp. 226-237.

[12]. J. L. Lovella, V. Haverdb, D. L. B. Juppb, et al., The Canopy Semi-analytic Pgap And Radiative Transfer (CanSPART) model: Validation using ground based lidar, *Agricultural and Forest Meteorology*, Vol. 158, Jun. 2012. pp. 1-12.

[13]. G. Zheng, L. Monika Moskal, Leaf Orientation Retrieval From Terrestrial Laser Scanning (TLS) Data, *IEEE Transactions on Geoscience and Remote Sensing*, Vol. 50, Issue 10, Oct. 2012. pp. 3970-3979.

[14]. H. Xu, N. Gossett, B. Q. Chen, Knowledge and Heuristic Based Modeling of Laser-Scanned Trees, *ACM Transactions on Graphics*, Vol. 26, Issue 4, Dec. 2007. pp. 1-19.

[15]. X. I. Liang, P. Litkey, J. Hyyppä, et al., Automatic Stem Mapping Using Single-Scan Terrestrial Laser Scanning, *IEEE Transactions on Geoscience and Remote Sensing*, Vol. 50, Issue 2, Feb. 2012, pp. 661-670.

[16]. T. R. Sam, K. S. Lawrence, Nonlinear Dimensionality Reduction by Locally Linear Embedding, *Science*, Dec. 2000, pp. 2323-2326.